Available online at www.sciencedirect.com
ScienceDirect
International Journal of Hydrogen Energy 32 (2007) 2494–2500
International Journal of HYDROGEN ENERGY
www.elsevier.com/locate/ijhydene

Characteristics of activation and anti-poisoning in an $LmNi_{4.8}Al_{0.2}$ hydrogen storage alloy

H.C. Lin[a,*], K.M. Lin[b], C.W. Sung[b], K.C. Wu[b]

[a]*Department of Materials Science and Engineering, National Taiwan University, Taipei, Taiwan*
[b]*Department of Materials Science and Engineering, Feng Chia University, Taichung, Taiwan*

Received 13 July 2006; received in revised form 26 October 2006; accepted 26 October 2006
Available online 11 December 2006

Abstract

The activation and anti-poisoning characteristics of $LmNi_{4.8}Al_{0.2}$ hydrogen storage alloy are investigated. The incubation period of $LmNi_{4.8}Al_{0.2}$ ranges from about 8 h to just a few minutes with activation temperatures of 20 and 80 °C, respectively. Poisoning effects become more problematic with a higher concentration of CO and a greater number of absorption/desorption cycles. The poisoning can be effectively inhibited by raising the temperature during hydrogen absorption/desorption. The poisoning by H_2S is less than that of CO. The poisoned $LmNi_{4.8}Al_{0.2}$ alloy can be successfully reactivated by purging with high purity hydrogen gas.

Keywords: $LmNi_{4.8}Al_{0.2}$ hydrogen storage alloy; Activation; Anti-poisoning

1. Introduction

Hydrogen is a clean, low polluting, renewable energy source [1]. It is considered to be a solution to replace the diminishing fossil fuels and beneficial in the protection of the global environment. From the application point of view, hydrogen storage is one of the keystones to "Hydrogen Economy". There are various methods for storing hydrogen, including high-pressure compressed gas, low-temperature liquid hydrogen, and solid-storage of metal hydrides in hydrogen storage alloys (HSAs). Of these methods, metal hydrides have recently attracted much attention due to their small volume, low equilibrium pressure and high safety. However, further investigation is required to improve the storage capacity of HSAs. Toxic impurities, such as CO, H_2S, NH_3 and CH_4, may be produced in hydrogen sources, particularly biological techniques [2]. Poisoning by these impurities can be detrimental to the HSAs, for example, they can reduce their hydrogen absorption rate and decrease the storage capacity after a few cycles of hydrogen absorption/desorption [3,4]. The development of HSAs with good anti-poisoning characteristics is, therefore, of great importance for the efficient storage of biologically produced hydrogen.

Due to its excellent performance in hydrogen storage, such as reversible and rapid reaction around normal temperature, controllable plateau pressure of 3–10 atm, high volumetric hydrogen density and good resistance to degradation, $LmNi_5$ is seen as one of the most promising candidates for hydrogen storage (Lm denotes La-rich misch metal) [5–7]. However, it is still necessary to promote the efficiency of $LmNi_5$ HSAs in the extraction and storage of the hydrogen gas from biological sources, in terms of obtaining a plateau pressure of less than 1 atm at room temperature and improvements of its anti-poisoning ability in the presence of impurities. According to previous researches [8,9], the plateau pressures below atmospheric pressure can be achieved through the partial substitution of Ni by Al in $LmNi_5$ alloys. However, an excessive addition of Al in the $LmNi_{5-x}Al_x$ alloys is seen to have some detrimental effects on the hydrogen storage characteristics, such as a steep plateau in the P–C–T curves, small capacity of hydrogen storage and large irreversibility during the hydrogen absorption/desorption cycle [10]. An alloy comprising of $LmNi_{4.8}Al_{0.2}$ is found to exhibit many excellent properties

* Corresponding author. Tel.: +886 2 3366 4532; fax: +886 2 2363 4562.
E-mail address: hclinntu@ntu.edu.tw (H.C. Lin).

0360-3199/$ - see front matter © 2006 International Association for Hydrogen Energy. Published by Elsevier Ltd. All rights reserved.
doi:10.1016/j.ijhydene.2006.10.064

of hydrogen storage, including high storage capacity of hydrogen, a flat and low-pressure plateau, and small irreversibility of hydrogen absorption/desorption [10]. In the present study, the activation and anti-poisoning performance of $LmNi_{4.8}Al_{0.2}$ are investigated in the presence of CO and H_2S impurities. Furthermore, a method of reactivating poisoned $LmNi_{4.8}Al_{0.2}$ alloy will also be assessed.

2. Experimental procedure

The $LmNi_{4.8}Al_{0.2}$ HSA was prepared by vacuum melting. The chemical compositions of the as-cast alloy, being analyzed using inductively coupled plasma atomic emission spectroscopy (ICP-AES), were found to be virtually the same as the nominal ones. The as-cast alloy was crushed below a 150 mesh and then annealed in an argon atmosphere at 950 °C for 12 h. The surface morphologies of the $LmNi_{4.8}Al_{0.2}$ particles were inspected by field emission gun scanning electron microscopy (FEG-SEM). The characteristics of hydrogen storage, including the activation, anti-poisoning ability and equilibrium pressure–concentration isotherms (P–C–T curves), were obtained using a computer controlled automatic "PCI Monitoring System" (GFE, Germany) with an accuracy of 1%. Toxic hydrogen sources were simulated by adding appropriate amounts of CO and H_2S impurities to pure hydrogen gas. The purging pressure was set to 45 atm during the process of hydrogen absorption.

3. Results and discussion

3.1. The activation characteristic of $LmNi_{4.8}Al_{0.2}$ alloy

During their preparation, the $LmNi_{4.8}Al_{0.2}$ particles will readily form an oxide layer on their surfaces. Thus, an activation process is necessary for $LmNi_{4.8}Al_{0.2}$ HSAs to efficiently absorb hydrogen gas. High purity and high pressure hydrogen gas is used to activate the $LmNi_{4.8}Al_{0.2}$ alloy. The hydrogen atoms gradually penetrate the oxide layer and subsequently diffuse into the crystal lattices. These hydrogen atoms occupy the interstitial sites in the crystal. Expansion of the lattice due to the occupation of hydrogen atoms leads to the splitting of the alloy particles into finer ones, referred to as pulverization [11,12]. As well as the reduction in particle size after activation, FEG-SEM images in Fig. 1(b) exhibit lots of microcracks on the newly created surfaces. The fresh surfaces created on these split particles are then very susceptible to hydrogen absorption.

Fig. 2(a) and (b) shows the activation curves and hydrogen absorption curves, respectively, at 20–80 °C for the $LmNi_{4.8}Al_{0.2}$ alloy. As shown in Fig. 2(a), the incubation period ranges from about 8 h to just a few minutes for 20 and 80 °C, respectively. This is attributed to the enhanced penetration of hydrogen atoms through the oxide layer and their increased diffusion rate into the crystal at higher temperatures. It can be seen from Fig. 2(a) that the activation rate increases rapidly at 40 °C and above. Moreover, the saturated hydrogen capacity in Fig. 2(a) is seen to decrease slightly with increasing activation temperature. This phenomenon can be related to the

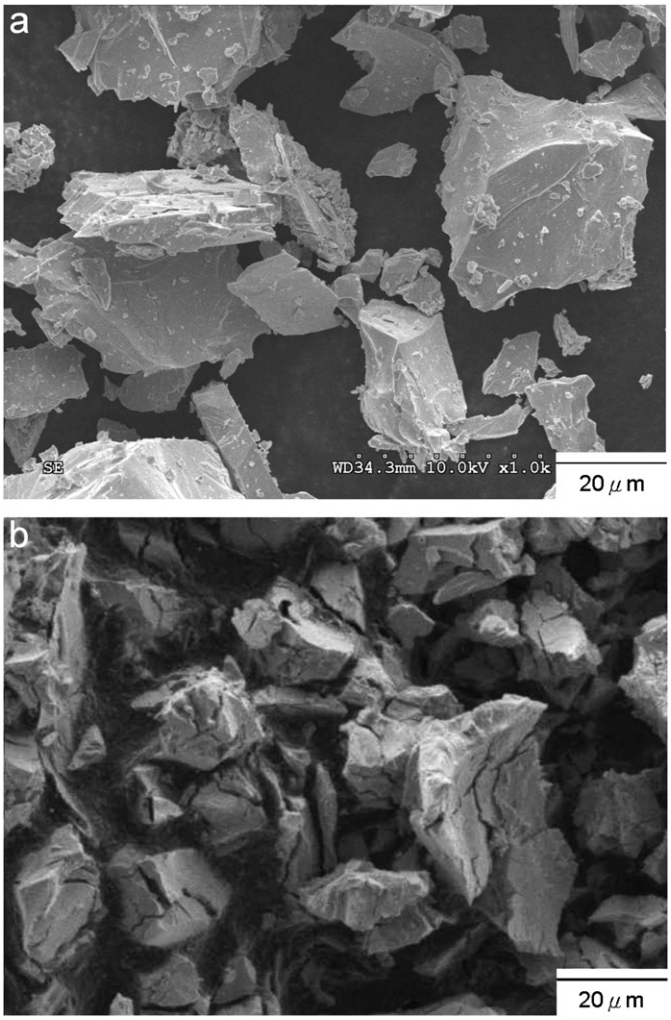

Fig. 1. The SEM images of the $LmNi_{4.8}Al_{0.2}$ alloy surface morphology (a) before and (b) after activation.

Van't Hoff relation [4,12]. Namely, the plateau region of metal hydride and its associated hydrogen capacity will decrease with increasing temperature. Fig. 2(b) shows the hydrogen absorption curves at 20–80 °C for the activated $LmNi_{4.8}Al_{0.2}$ alloy. Based on the Arrhenius equation and carefully examined data in Fig. 2(b), the activation energy of hydriding for the $LmNi_{4.8}Al_{0.2}$ alloy is calculated to be 32.6 kJ/g-atom H, which is similar to a reported value for $LmNi_5$ alloy (35.7 kJ/g-atom H) [13]. It is worthy to mention that the hydrogen absorption curves in Fig. 2(b) have even no obvious change after cyclic hydrogen absorption/desorption for the $LmNi_{4.8}Al_{0.2}$ alloy. This indicates that the $LmNi_{4.8}Al_{0.2}$ alloy will not exhibit the poisoning effect in the hydrogen source with high purity. This features is consistent with the results in a previous paper [6], which reported that the $LmNi_5$-based HSAs can still have 80% capacity even after 3000 cycles of hydrogen absorption/desorption.

Fig. 3 shows the P–C–T curves at 20–80 °C for the $LmNi_{4.8}Al_{0.2}$ alloy which has been subjected to activation. In Fig. 3, the plateau pressures of hydrogen absorption/desorption

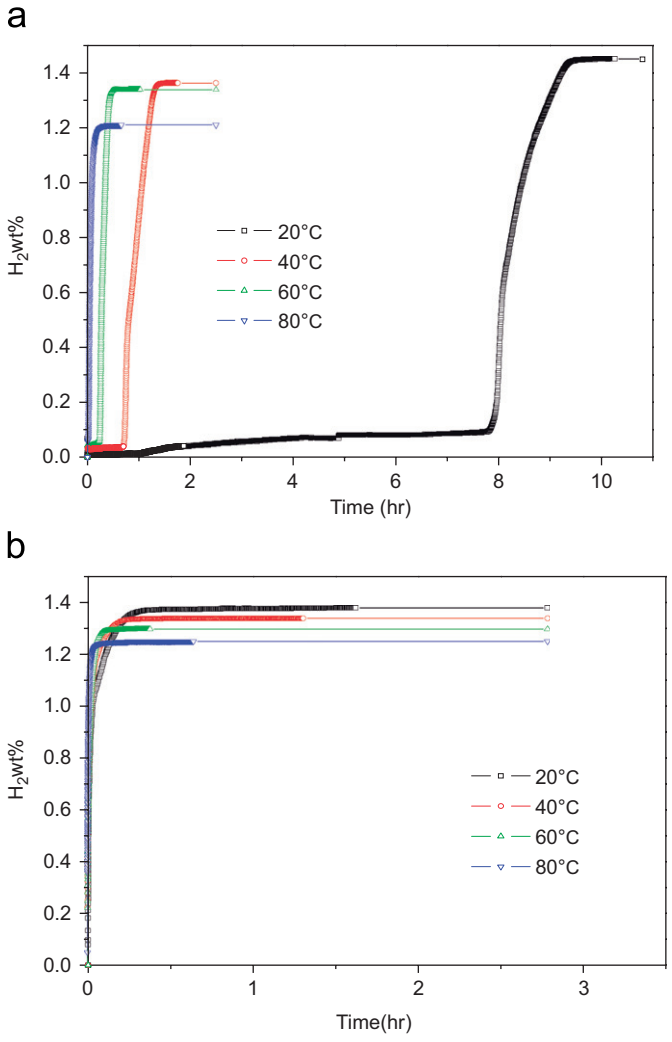

Fig. 2. The (a) activation curves and (b) hydrogen absorption curves at 20–80 °C for the $LmNi_{4.8}Al_{0.2}$ alloy.

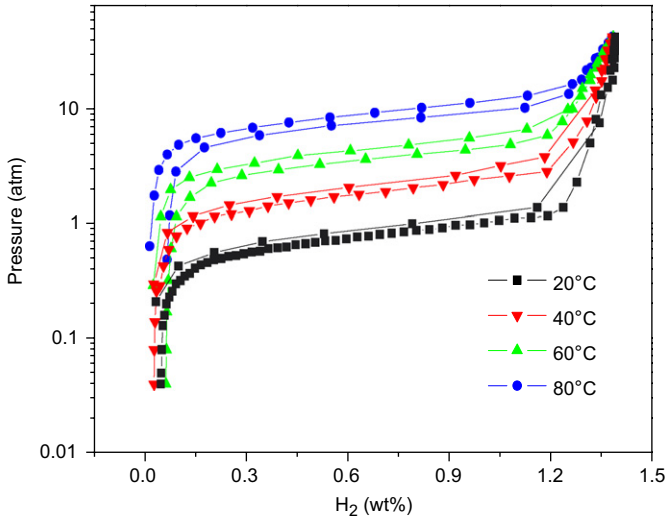

Fig. 3. The *P–C–T* curves at 20–80 °C for the $LmNi_{4.8}Al_{0.2}$ alloy that has been subjected to activation.

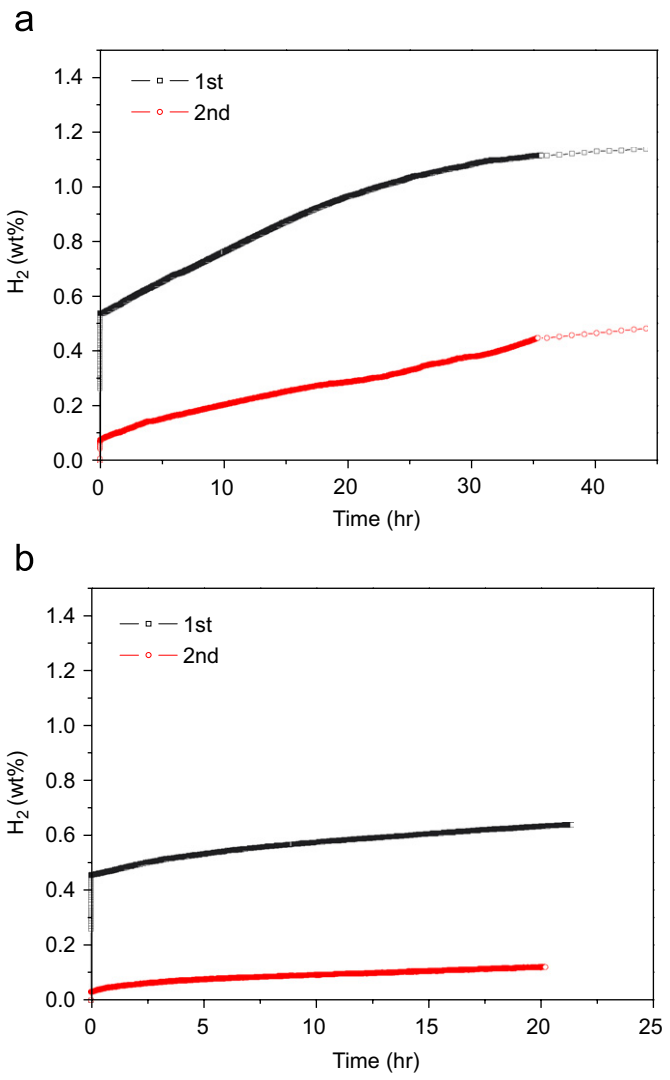

Fig. 4. The cyclic hydrogen absorption curves at 40 °C for the $LmNi_{4.8}Al_{0.2}$ alloy in hydrogen with (a) 300 and (b) 1000 ppm CO.

increases with increasing temperature and are in the region of 0.5–10 atm, which are suitable for practical applications. In addition, the hydrogen capacity still reaches approximately 1.35 wt%, which is a typical value for the $LmNi_5$-based HSAs.

3.2. The anti-poisoning characteristic of activated $LmNi_{4.8}Al_{0.2}$ alloy

Figs. 4 and 5 show the cyclic hydrogen absorption curves at 40 and 80 °C, respectively, for hydrogen sources with 300 and 1000 ppm CO. Fig. 6(a) and (b) shows the comparison of the first hydrogen absorption curves at various temperatures for $LmNi_{4.8}Al_{0.2}$ alloy in the presence of 300 and 1000 ppm CO, respectively. According to Figs. 4–6, the following observations can be made: (1) In the CO toxic hydrogen sources, the hydrogen absorption rate is much slower than in the pure hydrogen gas. (2) The hydrogen capacity decreases with the presence of CO. (3) The poisoning effect increases with an

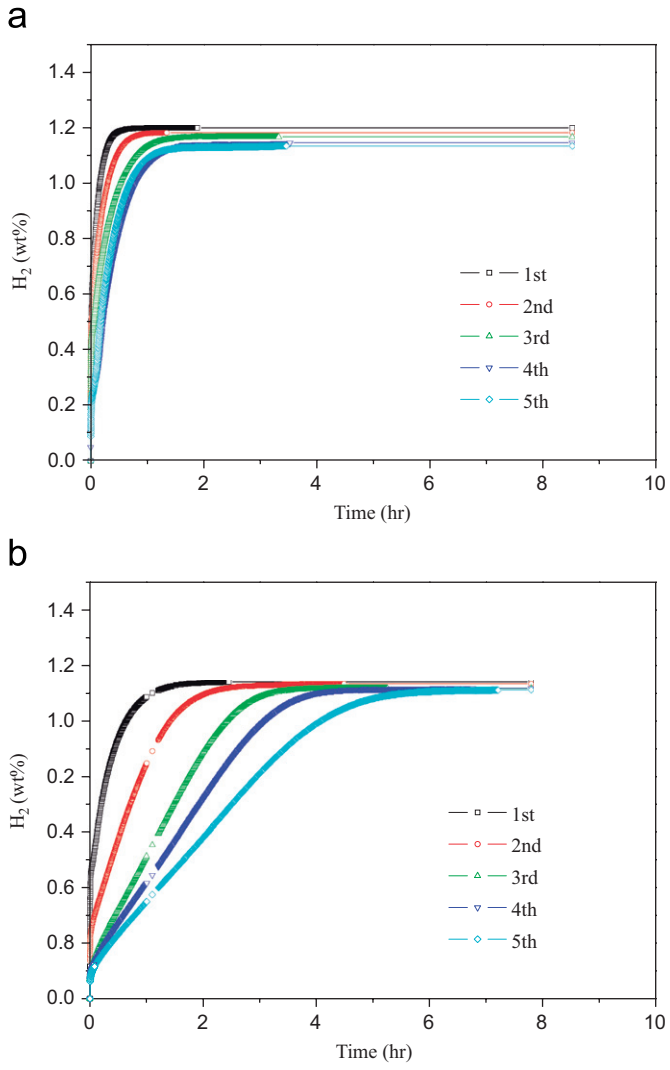

Fig. 5. The cyclic hydrogen absorption curves at 80 °C for the $LmNi_{4.8}Al_{0.2}$ alloy in hydrogen with (a) 300 and (b) 1000 ppm CO.

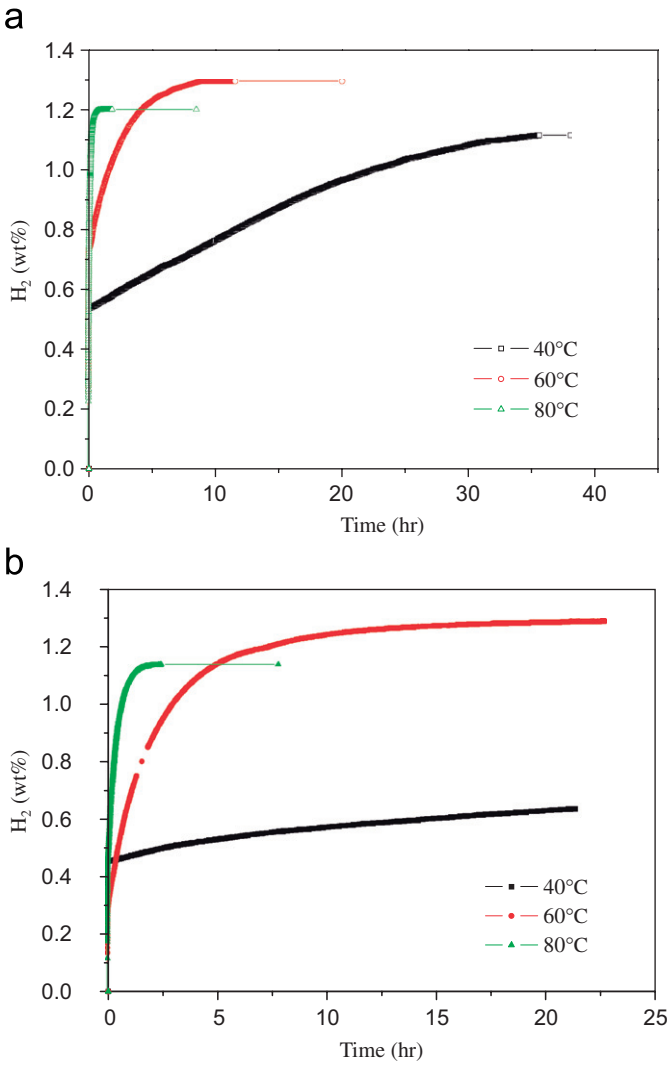

Fig. 6. The first hydrogen absorption curves of the $LmNi_{4.8}Al_{0.2}$ alloy at various temperatures in hydrogen with (a) 300 and (b) 1000 ppm CO.

increasing number of hydrogen absorption/desorption cycles. (4) The poisoning effect is greater at higher CO concentration. (5) At higher temperatures, the poisoning effect is less obvious; the absorption rate is still very fast at 80 °C even with 1000 ppm of CO. This indicates that CO impurity has a serious poisoning effect on the $LmNi_{4.8}Al_{0.2}$ alloy. As only hydrogen is permitted to enter the crystal lattices of the $LmNi_{4.8}Al_{0.2}$ alloy, the larger CO molecules can only be absorbed onto the surface. Furthermore, according to Hückel molecular orbitals for the metal–carbon–oxygen bonds [14], there exists a partially filled π-molecular orbital which increases the metal–carbon bond strength but decreases with the carbon–oxygen bond strength. These CO molecules will accumulate on the surface of the $LmNi_{4.8}Al_{0.2}$ particles and hinder the entry of hydrogen atoms into the crystal lattice, hence, reducing the ability of hydrogen absorption. The coverage of the surface will be higher with CO concentration and the number of cycles. Hydrogen absorption/desorption at elevated temperatures, however, will allow the surface bonds with CO molecules (i.e., the metal–carbon bonds) to be more easily broken. This will in turn increase the probability of hydrogen to enter the crystal lattices. Additionally, the reaction between CO and hydrogen, to form CH_4 and O_2, will be enhanced at higher temperatures. These CH_4 and O_2 gases are known to be less toxic for the $LmNi_{4.8}Al_{0.2}$alloy [3,15], and the poisoning phenomenon is partially prevented. These aforementioned factors may all have a significant contribution to the efficiency of hydrogen absorption at different temperatures.

The XRD patterns of the $LmNi_{4.8}Al_{0.2}$ alloy after 5 hydrogen absorption/desorption cycles at 60 °C in the presence of 1000 ppm CO, are shown in Fig. 7. Peaks relating to $LmNi_5H_{5.6}$ hydrides can be seen. This suggests that the CO molecules adhered to the surface of the alloy hinder the release of hydrogen atoms during the process of hydrogen desorption, resulting in a large amount of $LmNi_5H_{5.6}$ hydrides been retained in the crystal lattices. The residual $LmNi_5H_{5.6}$ will limit hydrogen absorption in the following cycles, therefore, reducing the adsorption rate and capacity of

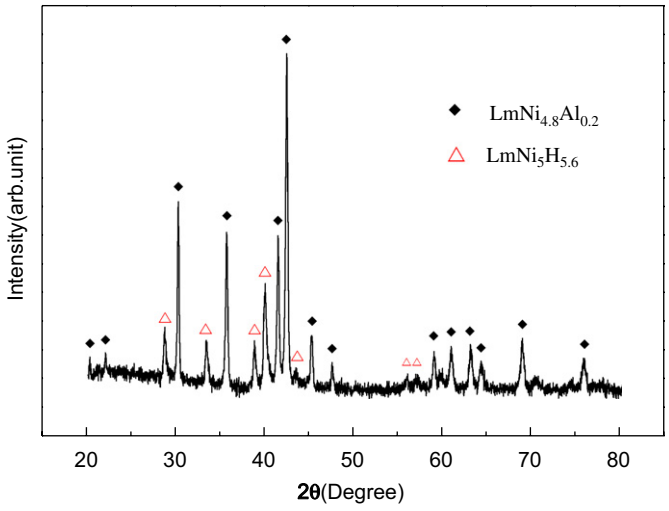

Fig. 7. XRD patterns of the $LmNi_{4.8}Al_{0.2}$ alloy after 5 cycles of hydrogen absorption/desorption at 60 °C in hydrogen with 1000 ppm CO.

hydrogen. These considerations are consistent with the *P–C–T* measurements.

The influence of CO impurity on the desorption behavior of the $LmNi_{4.8}Al_{0.2}$ alloy is examined by subsequently desorbing hydrogen at 40 and 80 °C in the presence of 1000 ppm CO, after absorption at 80 °C. From the results presented in Fig. 8(a) it can be seen that, at a desorbing temperature of 40 °C, the saturated hydrogen capacity decreases rapidly with increasing number of hydrogen absorption/desorption cycles. This suggests that CO molecules adhered to the surface of the alloy hinder the desorption of hydrogen at 40 °C. Hence, hydrogen absorption is decreased significantly in the following cycles due to the presence of residual $LmNi_5H_{5.6}$ hydrides. For a desorption temperature of 80 °C, however, the bonding between the CO molecules and the surface of the alloy can be broken easily. This allows a more complete release of the hydrogen atoms from the crystal lattices, as shown in Fig. 8(b), which is analogous to hydrogen absorption at 80 °C. Hence, even after 5 cycles of adsorption/desorption in a 1000 ppm CO toxic hydrogen source a high saturation capacity is maintained.

Fig. 9(a)–(c) shows the cyclic hydrogen absorption curves at 40, 60 and 80 °C, respectively, for the $LmNi_{4.8}Al_{0.2}$ alloy with the presence of either 1000 ppm CO or 1000 ppm H_2S. It is seen in Fig. 9 that the poisoning effect of H_2S impurity is considerably less than that of CO impurity at all temperatures of the hydrogen absorption/desorption. A relatively high hydrogen absorption rate and saturated hydrogen capacity is maintained, even after many cycles of hydrogen absorption/desorption, with the presence of 1000 ppm H_2S. The difference between the poisoning effects of CO and H_2S impurities can be explained as follows. As above mentioned, there exists a partially filled partially filled π-molecular orbital which can increase the strength of the metal–carbon bonds. These CO molecules adhered to the surface of the alloy hinder the entry of hydrogen atoms into the particles crystal. However, for the H_2S molecule, the S atom

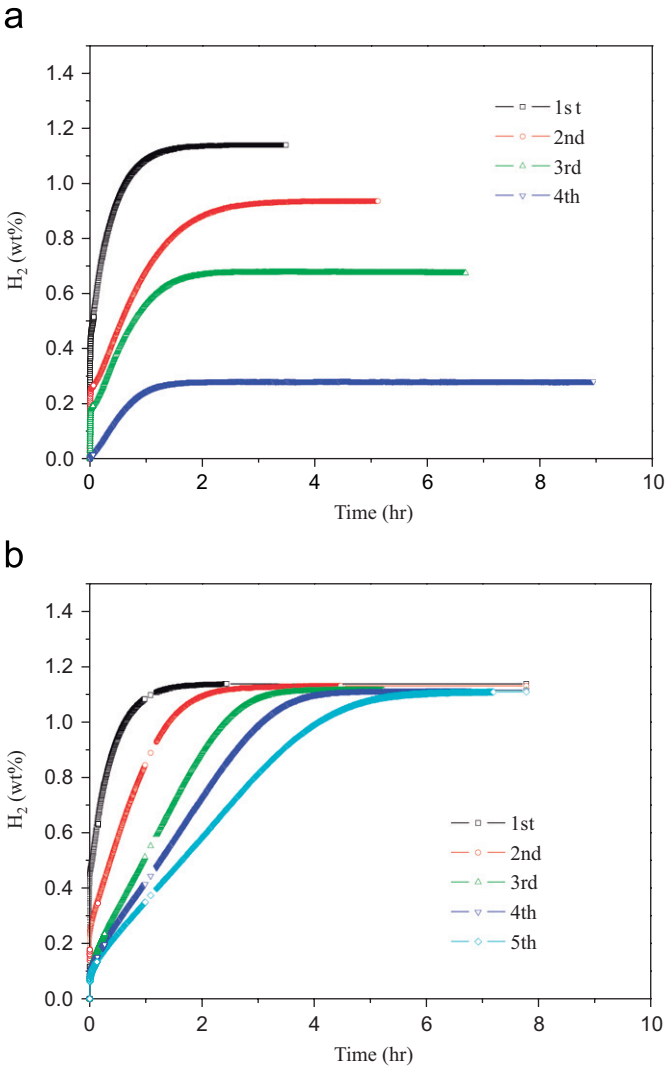

Fig. 8. The hydrogen absorption behavior for $LmNi_{4.8}Al_{0.2}$ alloy, which has been subjected to absorption of hydrogen at 80 °C and subsequent desorption at (a) 40 °C and (b) 80 °C in the presence of 1000 ppm CO.

has only two empty valences, which are exhausted completely in the bonding with the two H atoms. Hence, the H_2S molecules can only adhere to the surface by weak van der Waals bonding. It is known that these van der Waals bonded species do not effectively hinder hydrogen adsorption. As a result the poisoning effect in the H_2S toxic hydrogen source is less obvious than in the case of CO.

After the cyclic hydrogen absorption/desorption in the toxic hydrogen sources, the $LmNi_{4.8}Al_{0.2}$ alloy will lose some of its ability to efficiently absorb hydrogen. It is therefore worthwhile examining the re-activation process for poisoned $LmNi_{4.8}Al_{0.2}$ particles. Thus, after 5 poisoning cycles in 1000 ppm CO toxic hydrogen gas at 60 °C, reactivation of the $LmNi_{4.8}Al_{0.2}$ alloy is assessed by purging it with 99.999% pure hydrogen gas at a pressure and temperature of 45 atm and 60 °C, respectively. The hydrogen absorption curves after the first and second reactivation cycles for the poisoned $LmNi_{4.8}Al_{0.2}$ alloy are shown in Fig. 10. It can be seen that the poisoned alloy particles

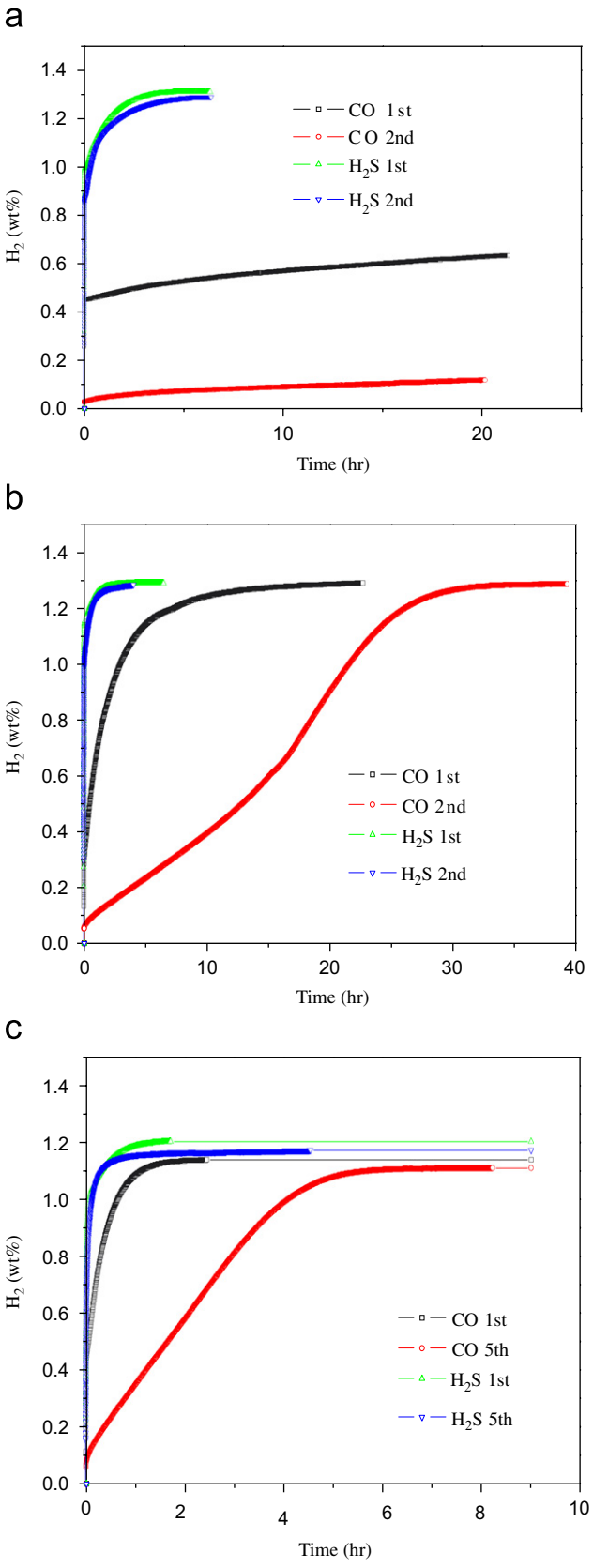

Fig. 9. The cyclic hydrogen absorption curves for the $LmNi_{4.8}Al_{0.2}$ alloy in both 1000 ppm CO and 1000 ppm H_2S toxic hydrogen sources at temperatures of (a) 40, (b) 60 and (c) 80 °C.

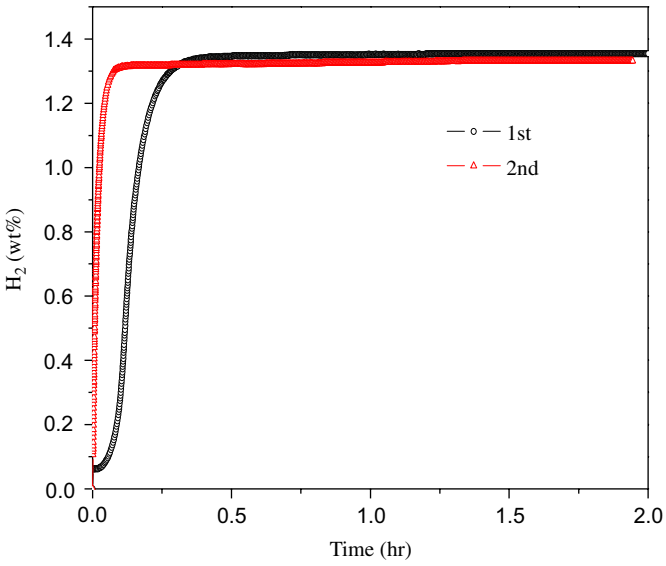

Fig. 10. The hydrogen absorption curves of the first and second reactivation cycles for CO poisoned $LmNi_{4.8}Al_{0.2}$ alloy.

have recovered most of their ability in absorbing hydrogen after the first reactivation cycle. During the second reactivation cycle, the hydrogen absorbing activity of $LmNi_{4.8}Al_{0.2}$ alloy is virtually fully recovered. The improved hydrogen adsorption capabilities after purging can be ascribed to the following: (1) Dilution and debonding of CO in the high pressure, pure hydrogen gas. (2) The pulverization process significantly increasing the amount of fresh surfaces. These factors will prevent the hindrance previously induced by CO poisoning and allow the hydrogen absorption rate to be increased significantly. This reflects the success of this method in the reactivation of CO poisoned $LmNi_{4.8}Al_{0.2}$ alloy particles.

4. Conclusions

1. At 20 °C the incubation period for activation of the $LmNi_{4.8}Al_{0.2}$ HSA was about 8 h. It sharply decreased at 40 °C, and was only a few minutes at an activation temperature of 80 °C. The activation energy of hydriding for the $LmNi_{4.8}Al_{0.2}$ alloy is estimated to be 32.6 kJ/g-atom H.
2. The $LmNi_{4.8}Al_{0.2}$ HSA was poisoned by the presence of CO during hydrogen absorption/desorption. A higher CO concentration and greater number of hydrogen absorption/desorption cycles increased the poisoning effects. Poisoning phenomenon was inhibited by raising the hydrogen absorption/desorption temperature.
3. The poisoning effect was considerably less for H_2S compared to CO.
4. Poisoned $LmNi_{4.8}Al_{0.2}$ alloy was successfully reactivated by purging in high pressure, pure hydrogen gas.

Acknowledgment

The authors would like to sincerely acknowledge the financial support of this study by Feng Chia University, Taiwan, Republic of China, under the Grant FCU-93GB27.

References

[1] Elam CC, Padro CEG, Sandrock G, Luzzi A, Lindblad P, Hagen EF. Int J Hydrogen Energy 2003;28:601–7.
[2] Levin DB, Pitt L, Love M. Int J Hydrogen Energy 2004;29:173–85.
[3] Han JI, Lee JY. J Less-Common Met 1989;52:319–27.
[4] Goodel PD. J Less-Common Met 1983;89:45–54.
[5] Yamamoto T, Inui H, Yamaguchi M. Mater Sci Eng A 2002;329–331: 367–71.
[6] Shen CC, Lee SM, Tang JC, Perng TP. J Alloys Compds 2003;356–357:800–3.
[7] Sato M, Yartys VA. J. Alloys Compds 2004;373:161–6.
[8] Mungole MN, Rai KN, Singh KP. Int J Hydrogen Energy 1991;16: 545–9.
[9] Joubet JM, Latroche M, Cerny R, Percheron-Guegan A, Yvon K. J Alloys Compds 2002;330–332:208–14.
[10] Sung CW, Master thesis, Fung Chia University, Taiwan; 2004 [in Chinese].
[11] Hout J, Bouaricha S, Boily S, Dodelet JP, Guay D, Schulz R. J Alloys Compds 1998;266:307–10.
[12] Sandrock G. J Alloys Compds 1999;293–295:877–88.
[13] Osovizky A, Bloch J, Mintz MH, Jacob I. J Alloys Compds 1996;2945:168–78.
[14] Blyholder G. J Phys Chem 1964; 2772–8.
[15] Eisemoerg FG, Goodell PD. J Less-Common Met 1983;89:55–62.